Mechanical Properties, Morphology, Flammability, and Thermokinetic Investigation of High-Density Polyethylene/Jatropha Deoiled Cake Composites

T. Elshaarani,[1] Z. Yaakob,[1] M. D. Khairul Zaman,[2] M. Mohammad,[1] S. R. S. Abdullah[1]

[1]*Department of Chemical and Process Engineering, Universiti Kebangsaan Malaysia (UKM), Bangi 43600, Selangor, Malaysia*
[2]*Radiation Processing Technology Division, Malaysia Nuclear Agency (Nuclear Malaysia), Bangi 43000 Kajang, Malaysia*

ABSTRACT: High-density polyethylene (HDPE)/jatropha deoiled cake (JOC) composites were fabricated by melt compounding; the molded specimens were tested for their tensile properties and water absorption. The thermal properties were investigated with thermogravimetry (TG) analysis, differential scanning microscopy (DSC), and limiting oxygen index testing. The degradation kinetic parameters were calculated with the Friedman and Freeman–Carroll models. The morphology of the tensile fractured composites was investigated by scanning electron microscopy. The results show that the introduction of JOC significantly reduced the tensile strength, percentage elongation at break, and modulus. On the one hand, JOC increased the water uptake. The TG and differential TG of JOC showed that the thermal degradation took place in two stages. The neat HDPE revealed a single degradation stage, whereas the blend showed three degradation stages. The composites' initial degradation temperature decreased; however, the residue chars increased with increasing JOC content. The activation energies (E_a's) were lower in the case of the blends than that corresponding to HDPE. The DSC results showed decreases in the melting temperature and degree of crystallinity of the composites. A considerable enhancement of the flame-retardant properties was observed for the composites. These experimental results suggest a synergetic effect caused by the coprocessing of the two materials together. © 2012 Wiley Periodicals, Inc. J Appl Polym Sci 000: 000–000, 2012

Key words: activation energy; composites; mechanical properties

INTRODUCTION

Jatropha curcas (physic nut or purging nut) is a drought-resistant shrub or tree belonging to the family Euphorbiaceae. It is cultivated in Central and South America, South East Asia, India, and Africa.[1] Its abundance is elevating because of the physicochemical properties of jatropha oil seed and its potential as biodiesel feedstock and in surface-coating industries.[2,3] The extraction of oil from jatropha oilseeds and its conversion into biodiesel involves many complex processes. The cake obtained after oil extraction is the major byproduct and can be use as a source of bioenergy. The cake is also rich in nutrients, especially protein; the protein content is higher than that in soybean meal.[4] Except for lysine, all other essential amino acids in jatropha meal protein have been reported to be in higher concentrations than those suggested for preschool children by the food and agriculture organization (FAO) reference pattern.[5] The defatted cake contains 46% crude protein, 14.3% crude fiber, and 7.3% nitrogen.

One of the major problems arising for the coming years is the disposal of the nonedible cake after oil is expelled for biodiesel production. It is estimated that jatropha plantations will produce 1000 kg of seed-cake/hectare crop.[6] The presence of the cake in the open atmosphere will generate gases, such as CH_4, N_2O, H_2S, NH_3, CO_2, and volatile compounds. The cake can be used neither for animal feed nor directly as a biofertilizer in agricultural farming because of its toxic nature. Many attempts have been made to recycle jatropha deoiled cake (JOC); these studies have demonstrated that JOC can be used as a source of animal feed (after detoxification)[7] and in industrial applications, such as in glues, coatings, and films.[8] The cake is a source for biogas production through anaerobic digestion. It has a low content of nonvolatile solids, a high volatile solids content, and higher hydrogen and carbon contents.[9] The formation of liquid oil, gas rich in hydrogen, and charcoal by the thermal decomposition of JOC have been reported.[10] Staubmann et al.[11] obtained 0.446 m[3] of biogas

containing 70% CH_4/kg of dry seed press cake using pig manure as inoculums. Additionally, the higher ash content was an indication of a large amount of minerals.[4] Thus, JOC is applicable as a direct fertilizer; its mineral properties are comparable with those of other organic fertilizers with regard to its nitrogen, phosphorus, and potassium contents.[12] The bioconversion of cellulosic materials in the press cakes of jatropha oilseeds into ethanol with the methods of acid pretreatment have been reported.[13] JOC is also rich in cellulosic compounds, which can be considered an inexpensive substitute for heavy-metal adsorption in wastewater treatment. Recently, Garg et al.[14,15] used JOC to remove cadmium and chromium from aqueous solutions.

JOC also contains a lot of proteins and fibers, which could serve as a biodegradable filler for a thermoplastic matrix. The objective of this study was to determine a chemical composition of JOC, use it in biodegradable composites without external compatibilizers, and to investigate the mechanical properties, water absorption, morphology, and thermal properties of the pure JOC and the resulting composites. Manufacturing thermoplastic composites with agricultural residue as a filler in place of expensive inorganic fillers in coprocessing will reduce the composite cost. In addition, it will decrease the dependence on petroleum products, which have contributed to many environmental problems.

EXPERIMENTAL

Materials

The jatropha curcas seeds used in this study were obtained from Universiti Kebangsaan Malaysia jatropha plantation in Kuala Pilah, Negeri Sembilan, Malaysia, and high-density polyethylene (HDPE, extrusion grade) was obtained from PE Malaysia Sdn. Bhd. (Petaling Jaya, Selangor). A melt flow index of 0.33 g/10 min was determined according to the ASTM D 1238-79 at 190°C with a standard of 2.16 kg of HDPE. An electronic densimeter (model MD-200S, Mirage, Japan) was used to measure the density of HDPE at 0.956 g/dm^3 according to ASTM D 792-86 by its immersion in distilled water. The melting temperature (T_m) of 132°C was determined with a Mettler Toledo DSC-1 with a rate of 10°C/min.

Chemical characterizations of JOC

The chemical composition of the jatropha deoiled cake (e.g., moisture and ash contents) were determined according to FAO (1999 and 1990), and the nitrogen content was determined by the Kjeldahl method. The crude protein was calculated with a nitrogen conversion factor of 6.3 (association of official agricultural chemists (AOAC), 2000), and the total lipid content

TABLE I
Chemical Compositions of JOC and HDPE

Component	Jatropha cake (%)	HDPE
Moisture content	12.3	0[b]
Total ash	3	0[b]
Total lipid	3.4	
Crude protein	46	
Crude fiber	14.3	
Nitrogen content	7.3	0.55[b]
Carbon	52.30[a]	84.95[b]
Hydrogen	6.50[a]	14.30[b]
Oxygen	26.8[a]	0.2[b]
Volatile matter	79.20[a]	100[b]
Hemicellulose	17.47[a]	
Cellulose	56.31[a]	
Lignin	23.91[a]	

[a] Viboon and Duangduen.[19]
[b] Dharmendra et al.[20]

was calculated with the percentage of lipids in the dry weight of the seed cake from a chemically extracted cake. The chemical analysis results of JOC and HDPE are presented in Table I. For JOC, the main elements were carbon at 52.30 wt % and oxygen at 26.8%. The volatile compounds mainly consisted of organic compounds (JOC), with a reported value of 79.20 wt %.

Composites preparations

The jatropha seeds were dehulled, blended, and chemically deoiled with n-hexane at 55°C for 6 h. The deoiled cake was dried in a Heraeus oven (Thermoelectron Corp., Am Kalkberg, Osterode, Germany) at 60°C for 24 h, refined, and sieved at 50 mesh. The resulting powder was dried at 80°C in a vacuum oven for 24 h to eliminate the moisture content and stored in a desiccator before compounding. JOC was melt-compounded with HDPE with a Haake rheometer (Polydrive, Carlsruhe, Bundesland, Germany) at a mixing temperature of 145°C for 10 min and a rotor speed of 55 rpm. The melt-compounded mixtures were compression-molded in a Labtech hot and cold press (Bangkok, Bangkok, Thailand) under a constant pressure of 150 kg/cm^3 into sheets 1.0 mm thick for tensile tests at 145°C for 20 min; this was followed by cooling at room temperature for 5 min.

Tensile tests

Mechanical tests were carried out at 23°C and 50% humidity according to ASTM D 1822-L. Seven specimens from each composition were tested with an Instron universal mechanical testing machine (Norwood, MA) with a load of 1 kN and operating at a grip separation speed of 50 mm/min.

Water absorption

The water absorption test was applied according to ASTM standard test method D 570-90. The tensile

testing specimens were used for water absorption testing, and three specimens for each treatment were selected. The selected specimens were dried in an oven for 24 h at 105°C; this was followed by cooling in a desiccator and immediate weighing. The dried specimens were submerged in distilled water at 25°C for 2 and 26 h. After 2 h, the specimens were removed, dried, weighed, resubmerged, and weighed again for another 24 h with a similar procedure. Water absorption was calculated as a percentage of initial weight.[16]

Thermogravimetric analysis (TGA)

The thermal stability characteristic studies of the resultant composites were carried out with TGA (PerkinElmer Pyris 1 TGA, Briggeport Avenue Shelton, CT, USA) under N_2 gas at a flow rate of 20 mL/min. A weight of 4–6 mg was subjected to a heating rate of 10°C/min and scanned from 50 to 600°C. The variation in sample mass with respect to temperature change (TGA data) and its first derivative [differential thermogravimetry (DTG) data] was continuously collected.

Kinetics of thermal degradation

The thermal decomposition kinetics related to TGA could be determined with the basic rate equation of conversion under a nitrogen atmosphere:

$$\frac{d\alpha}{dt} = Z(1-\alpha)^n e^{(-E/RT)} \qquad (1)$$

where α and $d\alpha/dt$ are the weight and weight loss rate at time t, respectively; Z, n, and E_a are the frequency factor (1/s), the decomposition reaction order, and the activation energy (J/mol), respectively; R is the gas constant (8.31447 J mol^{-1} K^{-1}); and T is the absolute temperature (K).

Freeman–Carroll method

This is a natural logarithmic differential form of eq. (1) with the rating of weight loss at different temperatures.[17] The formula is as follows:

$$\frac{\Delta \ln\left(\frac{d\alpha}{dt}\right)}{\Delta \ln(1-\alpha)} = n - E_a \left[\frac{\Delta\left(\frac{1}{T}\right)}{\Delta \ln(1-\alpha)}\right] \qquad (2)$$

A straight line will be obtained when one plots the following:

$$\Delta \ln(d\alpha/dt)/\ln(1-\alpha) \text{ versus } \Delta[1/T\,\Delta \ln(1-\alpha)]$$

The slope value is $-E_a/R$, and the intercept is n. The value of Z can be calculated with eq. (1), and the values of n and E_a can be obtained from eq. (2).

Friedman method

The Friedman technique is a single-heating-rate treatment method for thermogravimetry (TG) and DTG curves for determining the kinetic parameters of thermal decomposition and is as follows:[18]

$$\ln\left(\frac{d\alpha}{dt}\right) = \ln Z + n \ln(1-\alpha) - \frac{E_a}{RT} \qquad (3)$$

The E_a value can be obtained from the slope of the plot of ln $(d\alpha/dt)$ against $1/T$ for a constant α; n can be determined from the maximum slope (E_a/R) of the plot of Ln$(1 - \alpha)$ against $1/T$. Then, the Ln Z value can be obtained through eq. (1) at a certain temperature.

Differential scanning calorimetry (DSC)

The thermal analyses [e.g., crystallization temperature (T_c), T_m, and crystallization and melting enthalpies $(\Delta H_c$ and ΔH_m, respectively)] of the crystallization behavior of HDPE in the composite were carried out with a differential scanning calorimeter (Mettler–Toledo, DSC 1, STAR e System, Schwerzenbach, Zurich, Switzerland). The samples (ca. 6 mg each) were taken and placed in aluminum capsules. Each sample was heated from 50 to 210°C, maintained at this temperature for 5 min at a heating rate of 10°C/min, and cooled to 50°C. Finally, the heating curves of the samples were obtained by heating from 50 to 210°C at the same rate. The temperature and energy calibration was achieved by an indium standard under identical analytical conditions of the HDPE samples.

Fourier transform infrared spectroscopy

The FTIR spectra of the virgin HDPE and untreated jatropha cake–HDPE composite were obtained with a Thermo Fisher Nicolet 6700 FTIR spectrometer (Waltham, MA, USA) with CsI optics. Each sample was obtained by 32 consecutive scans with a resolution of 4 cm^{-1}; the samples were prepared with the ATR method within the range 400–4000 cm^{-1}.

Limiting oxygen index (LOI)

The flammability behavior of the neat HDPE and its composites was evaluated by the determination of their LOIs according to ASTM D 2863. Compression-molded plates with dimensions of $142 \times 52 \times 1$ mm^3 were held vertically in an FTA flammability apparatus (Stanton Redcroft, United Kingdom, London).

Morphological studies

The morphology of the selected samples was examined with scanning electron microscopy (SEM; Philips

TABLE II
Tensile Properties of the HDPE/JOC Composites

Jatropha cake content (%)	Tensile strength (MPa)	Young modulus (MPa)	Elongation at break (%)
0	29.533 ± 0.20	349.396 ± 8	111
10	25.352 ± 0.04	286.000 ± 9	23.7
20	21.773 ± 0.04	245.980 ± 4	18.1
30	17.949 ± 0.6	233.997 ± 9	14.3
40	13.563 ± 0.1	164.55 ± 10	14.2
50	12.832 ± 0.4	154.387 ± 6	12.6

XL30, North Billerica, Ma, USA) at an accelerating voltage of 20 EV. The side surface of the dumbbell specimens was studied after they were stretched at a 50 mm/min strain rate and 100% elongation. The fracture surface was coated with gold before SEM examination.

RESULTS AND DISCUSSION

Mechanical properties of the jatropha oil cake composites

The variation of tensile strength as a function of cake loading is shown in Table II. It is shown that the tensile strength decreased when the polymer matrix was filled with jatropha cake. The composite seemed to lose most of its strength linearly with increasing JOC from 10 to 50 wt % from 25.5 to 12.9 MPa, respectively; this represented a 56.6% decrease over unfilled HDPE for 50% cake loading. Similar findings were reported by Jacob et al.,[21] who studied blends made of soy isolate, soy concentrate, and soy flour with polyesters. His results showed that the mechanical properties of the composites decreased when the unmodified polyester was filled with proteins. Another result showed that the incorporation of JOC in styrene–butadiene rubber reduced its tensile strength.[22] The same trends have been reported by Yam et al.,[23] Selke et al.,[24] and Raj et al.,s[25] who studied both recycled and pure polyethylene–wood composites. Their data showed that the tensile strength decreased with increasing fiber content. The depression in the tensile strength was attributed to the poor adhesion between the hydrophobic HDPE and the hydrophilic jatropha cake. Additionally, the processing condition may have destroyed the cake fibers during the fiber and polymeric matrix melt compounding.[23]

The elastic modulus for the composite decreased slightly with increased JOC content. Arvanitoyannis et al.[26] reported lower elastic modulus values for low-density polyethylene (LDPE)–wheat starch extruded films with increased starch concentration. Obuz et al.[27] reported a reduction in the elastic modulus with increased sorghum flour or wheat gluten level in LDPE–sorghum flour or LDPE–wheat gluten extruded sheets. The decrease in elastic modulus

with filler addition could be explained by changes in the composite yielding behavior. Fillers modify the ductile polymers' stress–strain curve shape because of the crazing or dewetting effect. The adhesion between the filler and matrix was probably lost; this led to a significant decrease in the elastic modulus of the composite. From the table, it is obvious that the composite elongation decreased gradually with increasing JOC content because of the increased stiffness provided by the cake. It is necessary to modify HDPE with a polar group, such as a maleic anhydride, to enhance the adhesion between the composite components to increase the scope of these composites and their application in various fields, such as in the automotive and packaging industries.

Water absorption

The variation of water absorption of the HDPE/JOC composites for the melt-mixed composites was studied. Figure 1 shows a significant in the amount of water absorbed at various cake loadings. The percentage of the water uptake slightly decreased with increasing cake content. SEM confirmed that the poor dispersion and wettability of the cake in the matrix increased the gaps and flow of the composite interface. Jatropha cake contains many functional groups susceptible to water, including hydroxyl and amide groups. There were three main regions in the composites where the water could reside in, that is, the lumen, cell wall (of the fiber and cellulosic materials in the cake), and the gap between the cake and the matrix.[28,29] These three regions increased with increasing cake content at higher fiber content; as a result, the amount of water absorbed increased. The composites containing higher cake contents (40 and 50%) showed a significant increase in the percentage of water absorbed. This could have been due to agglomeration of the cake during melt compounding of the composite, which made many holes between
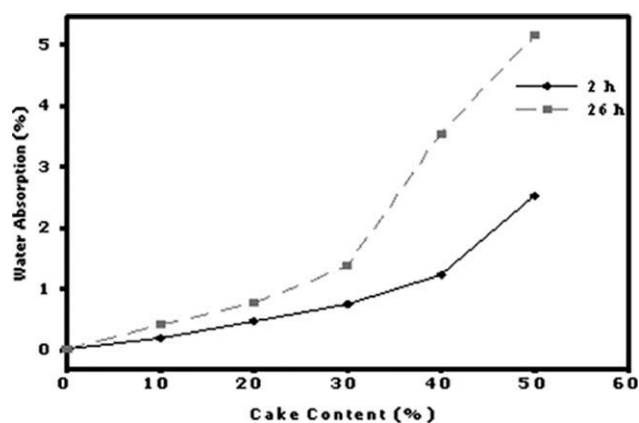

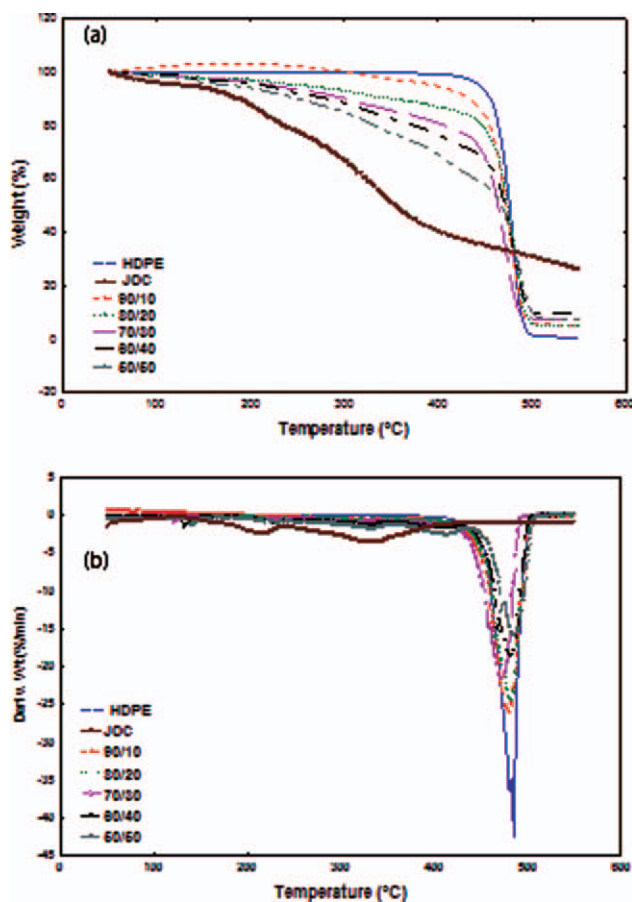Figure 1   Water absorption of the HDPE/JOC composites.

Figure 2 Thermograms of JOC, HDPE, and HDPE/JOC: (a) TGA and (b) Differential thermogravimetry analysis (DTGA) at a heating rate of 10°C/min in an N_2 atmosphere. [Color figure can be viewed in the online issue, which is available at wileyonlinelibrary.com.]

the matrix and the cake. Similar findings were also reported.[30]

TGA

Figure 2(a,b) depicts the TG decomposition process of the isolated materials (JOC and polyethylene) and

their blends. The corresponding data are listed in Table III. As can be observed from the graph, the thermal decomposition of JOC started at a lower temperature with an initial degradation temperature (T_i) of 174°C, whereas the decomposition of virgin HDPE started at a T_i of 483°C, and a nearly 100% decomposition occurred at about 500°C. From the table, it is apparent that the T_i for the composites was lower than that for the pure HDPE and higher than that of the pure JOC. The increase in cake content in the composites shifted T_i to a lower value. These were logical consequences of the lower thermal stability of jatropha cake. Similar findings were reported by Dharmendra et al.[20]

The DTG curve in Figure 2(b) indicates that a single degradation peak of neat HDPE appeared in the temperature range (TR) between 400 and 500°C with a maximum degradation temperature (T_{max}) of 483°C. It initiated primary thermal scissions of C—C chain bonds accompanied by a transfer of hydrogen at the site of scission, as reported in the literature. Two degradation processes were observed in the decomposition of JOC; these processes were a result of the degradation of three major constituents, that is, hemicellulose, cellulose and lignin. This is common in all lignocellulosic materials. Hemicellulose is degraded at temperatures between 150 and 350°C, cellulose is degraded from 275 to 380°C, and lignin is degraded from 250 to 550°C.[31] All of the composites and pure JOC experienced an early weight loss at 105°C with small endotherms on the DTG curve of about 73°C due to the evolution of water from the cake. Similar findings were noted in sisal fibers.[32] DTG exhibited two distinct T_{max} values for JOC, one around 218°C with a TR between 120 and 240°C. It corresponded to a weight loss of about 15% and resulted mainly from the thermal degradation of hemicelluloses. The second major mass loss occurred at a TR between 242 and 450°C with a T_{max} around 330°C, accompanied by a 46% weight loss. This peak corresponded to the thermal degradation of cellulose

TABLE III
Thermal Degradation Temperatures and Residue Weights of HDPE, JOC, and Their Composites

Composition HDPE/JOC	T_i^a (°C)	First stage		Second stage		Third stage		Residue (%)[c]
		TR	T_{max}^b	TR	T_{max}^b	TR	T_{max}^b	
HDPE	456	380–505	483					0.3
JOC	174	120–240	218	240–460	333			25.5
90%	446	100–360	331	370–520	403			5
80%	351	120–260	140	260–385	328	385–520	481	5
70%	311	100–260	123	260–370	328	370–500	472	7.6
60%	268	100–350	135	350–430	328	430–505	479	9.5
50%	232	120–350	325	360–440	410	440–505	483.5	8

[a] Initial thermal degradation temperature.
[b] Fastest degradation temperature.
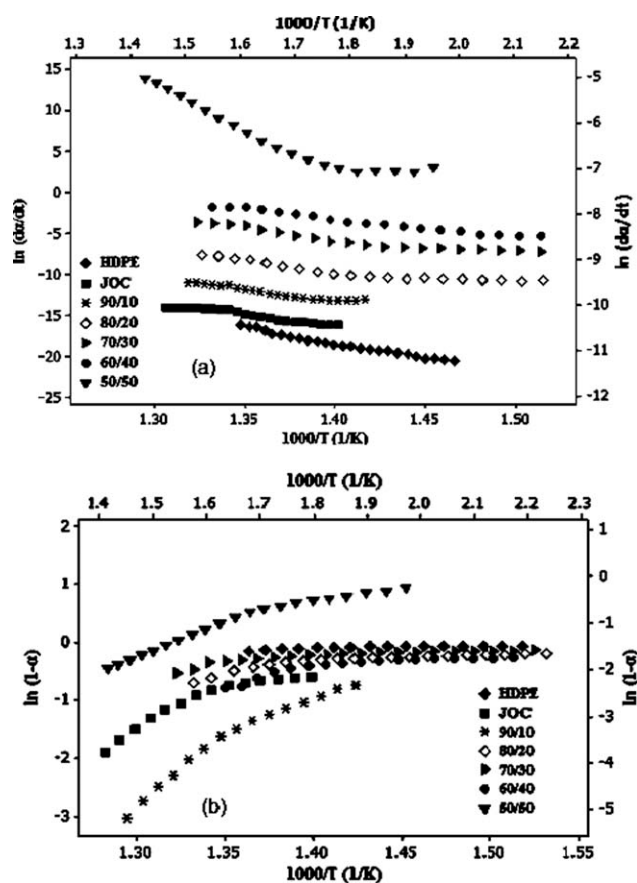[c] Residual weight was taken at 550°C.

Figure 3 Friedman plots of (a) $\ln(d\alpha/dt)$ versus $1/T$ and (b) $\ln(1 - \alpha)$ versus $1/T$ for the thermal degradation of HDPE, JOC, and their composites (heating rate = 10°C/min in nitrogen). *50/50 in the secondary axis: n constant values were added to separate the graphs.

due to dehydration and depolymerization; this led to the formation of flammable volatiles and char and left 25 wt % at 550°C. The lignin degraded slowly in a TR of 250–550°C.[33] After this sharp weight loss, there was a gradual but not appreciable weight loss. This observation gave us the perception that no major reactions existed above 550°C.

There were three degradation zones for the HDPE/JOC composites, except for the 90/10 composite, which exhibited only two degradation zones. The first degradation peak appeared at about 100–350°C. The second degradation peak appeared at about 240–420°C, where the evolution of light volatile compounds occurred. The strong third peak occurred between 370 and 520°C and indicated the degradation of thermoplastic.

During JOC degradation, many compounds, such as CO_2, CO, volatiles, bio-oil, and char, were produced because of dehydration and depolymerization reactions. Those compounds were considered to be responsible for accelerating the HDPE degradation in the HDPE/JOC blend. Similar observations were noticed in the thermal decomposition of polypropyl-

ene (PP)/wood flour composites.[34] This synergistic effect increased the weight loss rate and reduced the residue formation; thus, the TGA curves of the mixture were located between those of HDPE and JOC, with an early degradation stage of HDPE in the composite. Zhou et al.[35] also explained lower residue formation in the copyrolysis of Chinese pine wood sawdust with HDPE, LDPE, and PP. The residual weight of JOC at 550°C was about 25%. Although in the biomass–HDPE pyrolysis, very small quantities of the residue were in the range 5.0–9.0%, the suppression of residual formation was attributed to an increase in volatile production because they produced bio-oils from the early degradation of JOC, which interacted with HDPE and increased the volatile matter. Similar reasoning was put forth by Yogesh and Parimal.[36]

Further information on the thermal degradation of the HDPE, JOC, and their blends was determined with single-heating-rate methods, namely, the Friedman and Freeman–Carroll equations, at a heating rate of 10°C/min. It was not possible to use the same kinetic parameters to describe the thermal degradation over the entire TR accurately because of the differences in the nature of degradation between the composites and their individual components. From this point of view, the kinetic parameters for each degradation step were determined separately. The selected graphs plotted from the selected TR corresponded to the main thermal decomposition region for each sample.

Figure 3 depicts the relationship given by Friedman, whereas Figure 4 shows the relation of eq. (3). The calculated values of E, n, and Ln Z derived from the aforementioned linear plots are summarized in Table IV.

Table IV shows the tabulated values of E_a. E_a and the pre-exponential factor (Ln Z) for JOC determined by the Friedman method were 38 kJ/mol and 32 s^{-1}
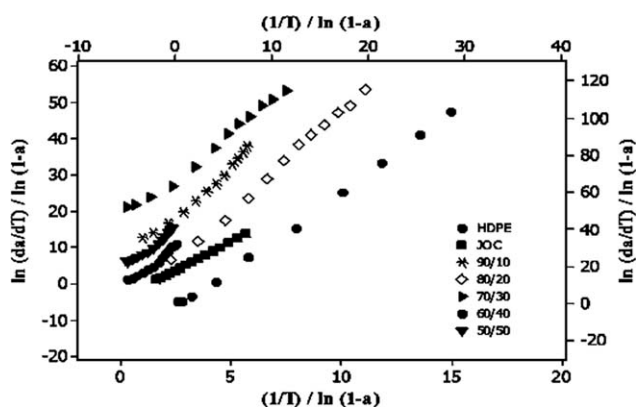

Figure 4 Freedman–Carroll plots of $\Delta \ln(d\alpha/dT)/\Delta \ln(1 - \alpha)$ versus $\Delta (1/T)/\ln(1 - \alpha)$ for the thermal degradation of HDPE, JOC, and their composites. (heating rate = 10°C/min in nitrogen) *HDPE curve in the secondary axis: n constant values were added to separate the graphs from each other.

TABLE IV
Kinetic Parameters of the Main Thermal Degradation Stage of HDPE, JOC, and Their Composites

Composition HDPE/JOC	Friedman			Freeman–Carroll		
	E_{a1}	E_{a2}	E_{a3}	E_{a1}	E_{a2}	E_{a3}
HDPE	315			34		
JOC	38	24		27	26	
90/10	36	190		25	26	
80/20	57	38	172	26	33	43
70/30	53	40	96	26	31	40
60/40	23	53	236	25	35	38
50/50	24	57	251	25	34	34
	n_1	n_2	n_3	n_1	n_2	n_3
HDPE	1			1.6		
JOC	7	0.8		5	0.2	
90/10	4.2	0.98		22	3.2	
80/20	38	10	1.1	30	9	4.7
70/30	38	18	4.5	31	5.5	2
60/40	4	2.5	1	10	0.5	1
50/50	6	3.9	1	8.6	0.2	0.6
	$\text{Ln } Z_1$	$\text{Ln } Z_2$	$\text{Ln } Z_3$	$\text{Ln } Z_1$	$\text{Ln } Z_2$	$\text{Ln } Z_3$
HDPE	311			30		
JOC	32	17		21	19	
90/10	28	181	102	20	18	
80/20	47	30	167	17	25	42
70/30	44	34	93	17	23	35
60/40	14	45	233	16	27	35
50/50	17	51	246	19	26	31

Heating rate = 10°C/min under nitrogen.

in the first degradation region and 24 kJ/mol and 17 s^{-1} for the second degradation region, respectively. With the Freeman–Carroll method, the calculated values were around 27 kJ/mol and 21 s^{-1} and 26 kJ/mol and 19 s^{-1} for the first and second regions, correspondingly. Ramiah[37] showed E_a values in the ranges of 150–250, 62–108, and 54–79 kJ/mol for cellulose, hemicellulose, and lignin. E_a values of 33 and 36 kJ/mol were reported for the thermal degradation of calotropis procera and baggasse,[38] respectively. E_a and Ln Z for HDPE were 315 kJ/mol and 311 s^{-1} in the case of the Friedman method and 34 kJ/mol and 30 s^{-1} in the case of Freeman–Carroll method, respectively. The reported E_a's in the literature for HDPE vary over a wide range. Sorum et al.[39] reported a value of 445 kJ/mol at heating rate of 10°C/min. Hee and Sea[40] reported tremendous variation in the kinetic parameters of PP, HDPE wastes, and their blends.

A three-step reaction was used to describe the copyrolysis process of the blends. The Friedman method led to apparent E_a's that fluctuated between 23 and 57 kJ/mol for the first stage, 24 and 190 kJ/mol for the second stage, and 96 and 251 kJ/mol for the last stage. On the other hand, the values of E_a calculated with the Freeman–Carroll method for the first, second, and third stages varied from 25 to 26, 26 to 35, and 34 to 43 kJ/mol, respec-

tively. Clearly, there were tremendous variations in the calculated E_a and Ln Z between the two methods; these were attributed to the difference in the mathematical approach used to calculate the kinetic parameters.[41] Dharmendra et al.,[20] who studied the synergic effects of HDPE with jatropha cake and karanja cake found that the E_a values of HDPE decomposition were 235–258 kJ/mol for the first stage with no further stage and JOC decomposition was 17–28 kJ/mol for the first stage and 48–60 kJ/mol for the second stage at heating rates of 5 and 20°C/min, respectively. He also found a reduction in E_a for the mixture. Similar results were obtained from the copyrolysis of Chinese pine wood sawdust with polyolefins, where three stages of the pyrolysis process were observed with E_a values varying from 107 to 128 kJ/mol for the first stage, 164 to 249 kJ/mol for the second stage, and 426 to 498 kJ/mol for the third stage.[35]

From the observation, we found that the E_a value for the blends was lower than that of the pure HDPE component. Aboulkas et al.[42] observed similar behavior during copyrolysis of olive residue with HDPE, and a reduction in the E_a of PP copyrolysis with calotropis procera was also reported.[43] The biomass can be visualized to synergistically reduce the E_a of HDPE degradation. During the pyrolysis, the biomass acts as a free-radical donor.[44] The produced radicals may attack the polyethylene and cause chain scission; thus, the overall E_a will be reduced. Higher values of E_a were noticed in the final stage, maybe because of the stronger energy needed for the bond scission of the polymer chains.[45]

As far as n is concerned (Table IV), the n values for thermal decomposition are different for the different thermal decomposition zone than the thermograms divided into three zones. The results show that the order of the reaction with the Friedman method at the low-temperature degradation zone (n_1) varied from 1 to 38. The order of reaction for the moderate temperature degradation zone (n_2) varied from 0.8 to 18, and the order of reaction for the higher temperature degradation zone (n_3) varied from 1 to 4.5. The values of n are an indication of the decomposition reaction rate. Higher values of n represent a slow reaction and vice versa. HDPE gave an n_1 with the Friedman method and a value of 1.6 with the Freeman method. These results agreed with those recorded by Ceamanos et al.[46]

DSC studies

DSC was used to study the thermal transitions that occurred during heating because of changes in enthalpy (ΔH) under an inert atmosphere. The DSC thermograms of JOC in Figure 5 show an exothermic transition at 97°C with an enthalpy of fusion of 132 J/g during the first heating cycle, which might
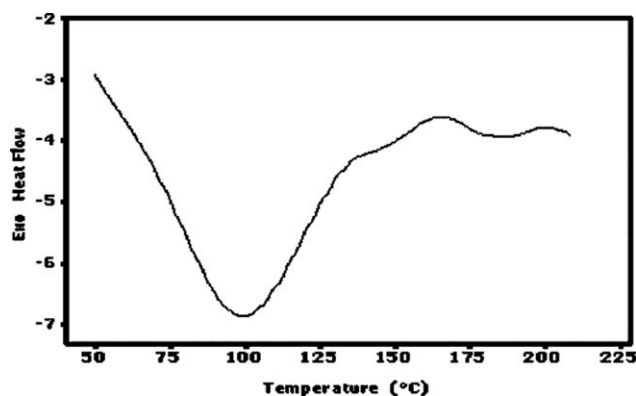
Figure 5 DSC thermogram of the jatropha cake.

have been due to the melting of the protein compounds in the jatropha cake. Similar results were recorded when soy protein/polyester blends, soy flour, soy protein concentrates, and soy isolates were examined with DSC; this indicated that T_m of soy protein was approximately 87–93°C.[47] The exothermic peak was followed by two endothermic transitions at 165 and 200°C with heats of fusion of 6.6 and 1.8 kJ/g. Typical DSC thermographs of HDPE and its composites with jatropha cake are demonstrated in Figure 6. In quantitative terms, the degree of crystallinity (X_c) of the HDPE matrix was evaluated from the following equation:

$$X_C = \frac{\Delta H_{\exp}}{\Delta H} \times \frac{1}{W_f} \times 100\% \tag{4}$$

where $\Delta H_{\exp}$ is the experimental heat of fusion or crystallization determined from DSC, ΔH is the melting heat of fusion or crystallization of a hypothetical fully crystalline HDPE (290 J/g),[48] and W_f is the weight fraction of HDPE in the composite. The DSC results of all neat matrices and composites are summarized in Table V. Calorimetric measurements (Table V) showed that the T_c of neat HDPE was 120.4. The addition of JOC had a negligible effect on T_c of the HDPE matrix. The T_c of HDPE deceased in the blends by 1°C, whereas the T_m for the composites was depressed by 1–4°C compared to HDPE. This indicated an improvement in the processing temperature of HDPE after it was filled with the cake.

Generally, the introduction of jatropha cake decreased the T_m of HDPE (Table V). This influence was significant when a higher cake content was used. The value of ΔH_m provided important information about the X_c of the composites, as shown in Table V. ΔH_m and ΔH_c of HDPE decreased gradually with increasing JOC content; the expected ΔH values showed high deviation from the obtained one. All of the composites, except the 50/50 composite, presented negative influences on X_c of HDPE. For example, the introduction of 10% JOC in the matrix

decreased X_c from 75% for the HDPE to 66%, whereas 40 wt % JOC was observed to reduce X_c to 62%. Yao et al.[49] found that rice straw fiber decreased the crystallization rate of HDPE and, consequently, resisted the recrystallization of HDPE. However, the composite's X_c increased slightly to 77% at 50 wt % cake loading; no significant change was observed at the 20 and 30 wt % JOC loadings. All of the composites showed a higher X_c than the theoretical one, with the largest deviation at 38% for the composites made of 50% JOC. The large deviation for the composites probably occurred because of the higher surface area of the cake.

LOI

LOI is defined as the minimum molar percentage of oxygen in a mixture of oxygen and nitrogen necessary to barely support flaming combustion of a material initially at room temperature under the conditions of the test method. It is determined by the volume ratio of the oxygen in the oxygen–nitrogen mixture at which the burned material still burns, that is

$$LOI = O_2/(O_2 + N_2)$$

The greater the LOI of a given material is, the lower is its flammability. The LOI values of the neat
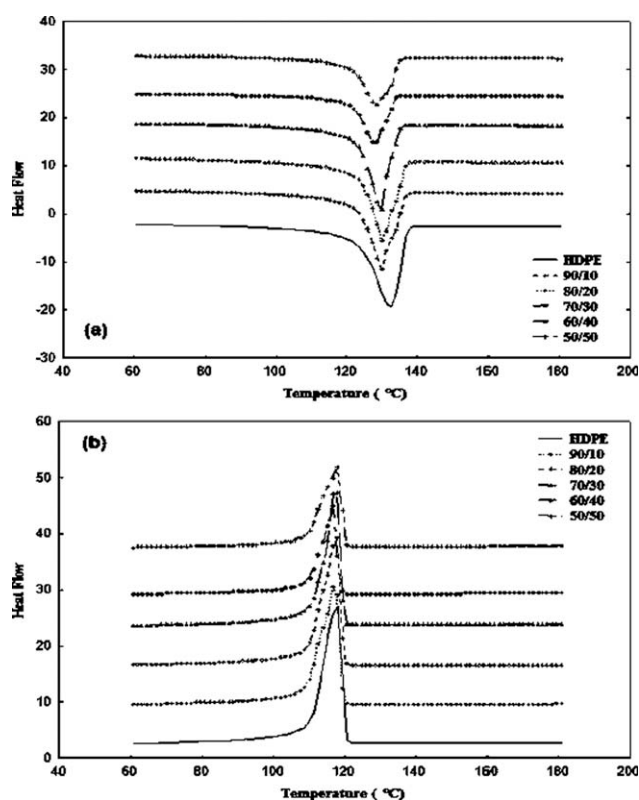

Figure 6 DSC thermograms of the (a) crystallization and (b) melting of the HDPE/JOC composite. The cooling and heating rate was 10°C/min.

TABLE V
DSC Analysis Results for HDPE and its Composites

HDPE/JOC blend	T_c (c)	ΔH_c (J/mol)	T_m (°C)	ΔH_m (J/mol)			X_c (%)		
				Obtained	Calculated[a]	Deviation	Obtained	Calculated[a,b]	Deviation
100/0	120.40	217	131.5	215	—	—	75	—	—
90/10	119.60	172	129	169	193	−24	66	58	+7%
80/20	119.84	174	129.5	172	172	0	75	59	+15%
70/30	119.73	151	129	149	150	−1	74	51	+22%
60/40	118.88	107	127.5	101	84	+17	62	23	+25%
50/50	118.94	112	127.7	111	107	+4	77	38	+38%

[a] The expected value depended on the HDPE percentage in the composite.
[b] The expected value were calculated on the basis of the experimental values of pure HDPE.

polymer and its composites are tabulated in Figure 7. As listed, HDPE had an LOI value equal to 17.8, whereas composites made of 10 and 30% JOC represented LOI values of 19.8 and 22%, respectively. Jia et al.[50] reported a value of 17.5% for pure HDPE. It is noteworthy that the composite made of 50% JOC had a relatively high LOI, with a value equal to 25.2%. Hence, the presence of the cake reduced the flammability of the HDPE, and the composites presented higher LOIs in comparison to the neat polymer. Apparently, there was a synergetic effect of JOC in enhancing the LOI of the HDPE composites. The results show a linear relationship between the char yield in the pyrolysis experiment in the TGA results (Table III) and the LOI with an increase in JOC content. Generally, polymers with a high char yield possess longer ignition times, lower heat release rates, and slower flame spread rates and generate less smoke and toxic gases than low char-forming polymers.[51,52]

The char layer may act as a thermal insulator because of its low thermal conductivity; in addition, char limits the access of oxygen from the atmosphere to the decomposing region. Furthermore, char can act as a barrier against the flow of volatiles from the decomposition zone. Finally, char can help retain the

structural integrity of a fire-damaged composite by holding the fibers in place after the polymer matrix has been degraded.[53] Certain flame-retarding elements present in the cake, such as phosphorus, will also increase the oxygen index.

FTIR analysis

Figure 8 shows the FTIR spectrum of HDPE and its composites. FTIR spectroscopy was used to characterize the surface functional groups and identify any new bonding generated after the blending of HDPE and JOC. The spectrum of HDPE showed a broad peak at 3290 cm^{-1}, which corresponded to the O—H stretching due to this H bonding in an alcohols and phenol compounds. The peak at 2914 cm^{-1} showed O—H stretching of carboxylic groups and C—H stretching of alkanes, the 2847-cm^{-1} peak corresponded to the existence of a carboxylic group, and the 1422- and 718-cm^{-1} peaks corresponded to the aromatic group. The composite of HDPE/JOC showed some new peaks at 1547, 1653, 1746, and 2319 cm^{-1}. These were probably due to the protein content in the cake represented by imide I (—CO—NH$_2$—) and amide II (—CO—NH—), where the peak at 1547 cm^{-1} corresponded to the N—O
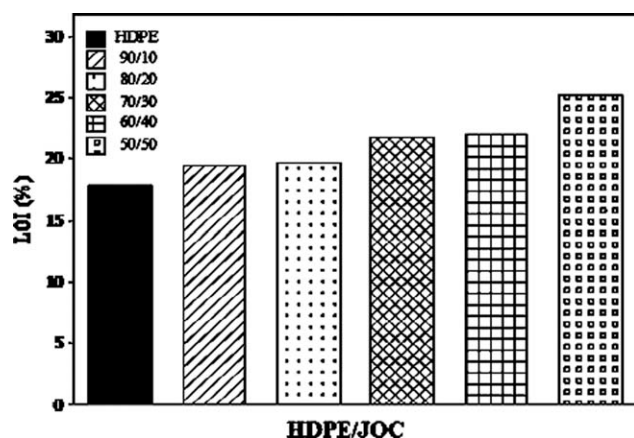

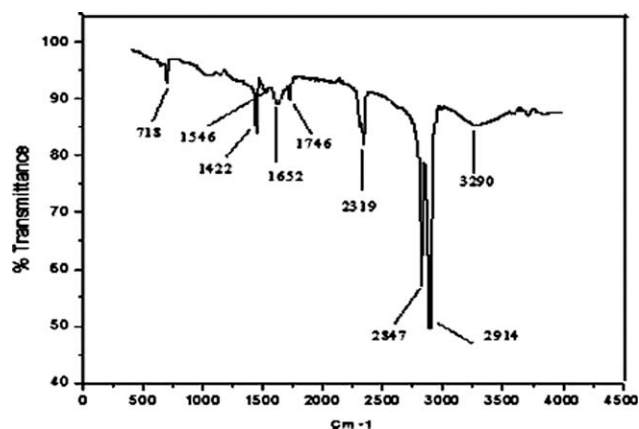Figure 7   LOI for the HDPE and HDPE/JOC composites.

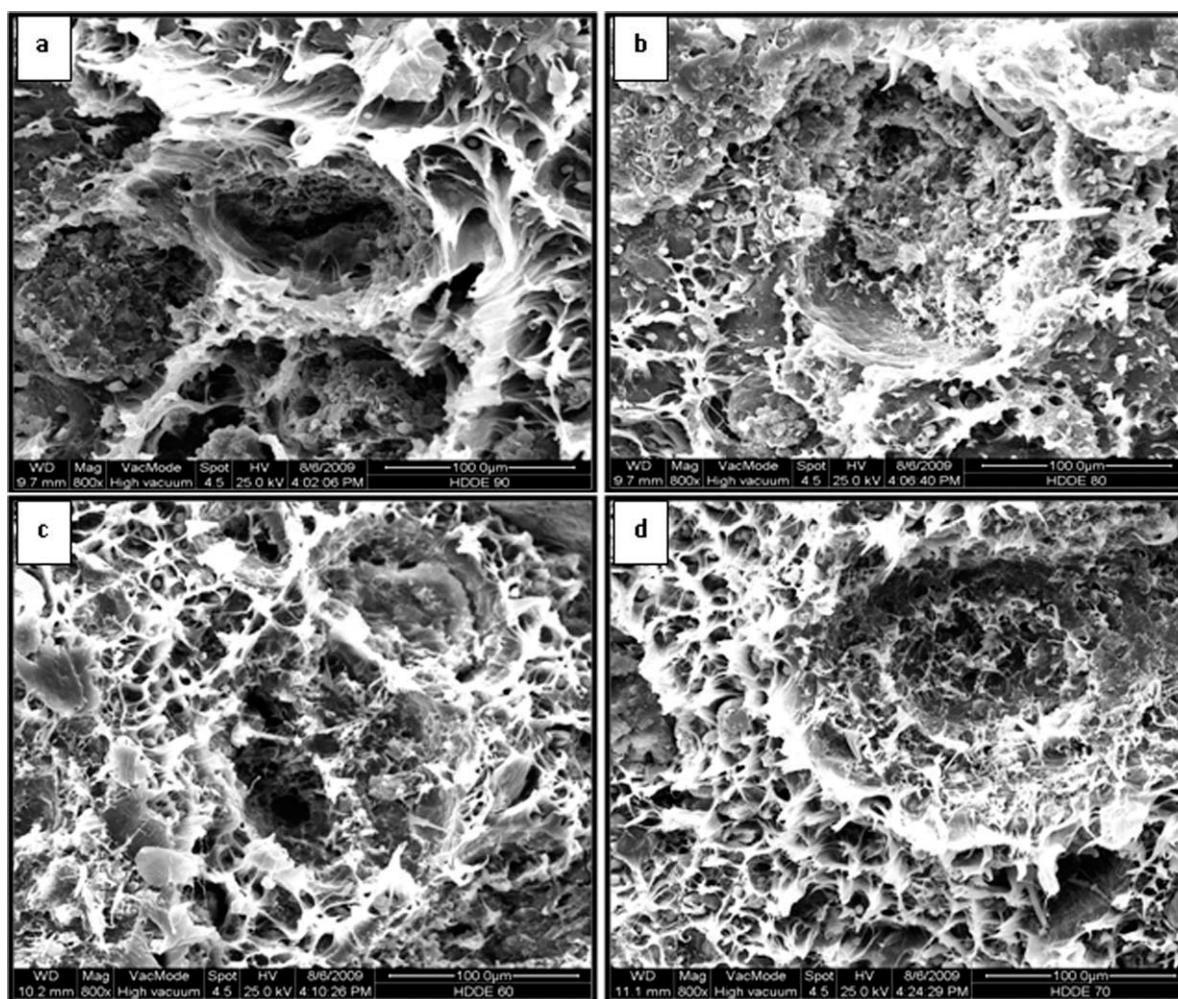

Figure 8   FTIR spectra of the HDPE/JOC composite.

Figure 9   SEM micrographs of (a) 10, (b) 20, (c) 30, and (d) 40% JOC.

asymmetric stretching of the nitro compound, the 1653-cm^{-1} peak corresponded to the alkene C=C vibrations, and that at 2319 cm^{-1} corresponded to acetonitrile. The shift in the amide II carbonyl group was due to the coupling of N—H bending and C—N stretching, whereas a carbonyl C=O stretching band appeared at 1746 cm^{-1} and was probably due to the jatropha oil spectrum (triglycerides) carbonyl group.[54]

Morphology of the bends

The fracture surface morphology of the tensile specimens is shown in Figure 9(a–d). As clearly seen, the cake was agglomerated and distributed in a large and broad size with many gaps between the cake and the polyethylene matrix. Those gaps were the result of poor dispersion and inadequate wetting of the fiber inside the matrix. This was probably due to incomplete interfacial bonding between the cake and the matrix during composite blending. Arib et al.[56] and Zahira et al.[55] reported similar results.

CONCLUSIONS

The mechanical, morphological, and thermal properties of HDPE/JOC composites were investigated. Decreases in the modulus and tensile strength were discovered with an increase of 50% JOC content. The TGA graphs showed a reduction in the residual weight for the composites compared to pure JOC, and DTG thermograms displayed three main thermal degradation peaks for the composites, whereas HDPE in its pure state showed a single degradation peak. The calculated E_a values of the HDPE/JOC blends in three pyrolysis stages with the Friedman method ranged from 24 to 57 kJ/mol for the first degradation stage and from 38 to 37 kJ/mol for the second stage, and for the last stage, it ranged from 96 to 251 kJ/mol. The composites showed a decrease in their thermal stability; the E_a at an early stage of degradation was lower than that calculated in the final degradation stage. This was because less energy was used to remove the loosely bound water and low-molecular-weight materials present in the latex. The reduction of in E_a and T_i with the increase

in cake content indicated a synergistic effect caused by the mixture of the jatropha cake with HDPE. The incorporation of JOC into the polymer matrix resulted in a notable increase in the LOI values. Jatropha cake decreased X_c of the matrix compared with that of the neat HDPE; the composite present lower peak T_c's. The results also show that 50 wt % cake loading increased X_c of HDPE. The degree of water absorption was increased by increases in the cake content and immersion time.

References

1. Schmook, B.; Seralta-Peraza, L. In Biofuels and Industrial Products from *Jatropha curcas*; Gübitz, G. M., Mittelbach, M., Trabi, M., Eds.; DBV: Graz, 1997.
2. Emil, A.; Zahira, Y.; Siti Kartom, K.; Manal, I.; Jumat, S. Eur J Sci Res 2009, 3, 29.
3. Emil, A.; Zahira, Y.; Satheesh Kumar, M. N.; Jahim, J. N.; Jumat, S. J Am Oil Chem Soc 2010, 87, 689.
4. Makkar, H. P.; Francis, G.; Becker, K. J Sci Food Agric 2008, 88, 1542.
5. Makkar, H. P. S.; Becker, K.; Schmook, B. Plant Foods Human Nutr 1998, 52, 31.
6. Mahanta, N.; Gupta, A.; Khare, S. K. Bioresour Technol 2008, 99, 1729.
7. Haas, W.; Mittelbach, M. Ind Crops Prod 2000, 12, 111.
8. Patel, V. C.; Varughese, J.; Krishnamoorthy, P. A.; Jain, R. C.; Singh, A. K.; Ramamoorty, M. J Appl Polym Sci 2008, 107, 1724.
9. Chandra, R.; Vijay, V. K.; Subbarao, P. M. V.; Khura, T. K. Appl Energy, to appear.
10. Atong, D.; Sricharoenchaikul, V. Mater Sci Forum 2007, 2127, 561.
11. Staubmann, R.; Foidl, G.; Foidl, N.; Gübitz, G. M.; Lafferty, R. M.; Valencia Arbizu, V. M. In Proceedings from the Symposium Jatropha 97, Managua, Nicaragua: Dbv-Verlag, Graz, Austria, 1997; p 123.
12. Delgado Montoya, J. L.; Parado, T. E. In New Crops for Food and Industry; Wickens, G., Haq, N., Day, P., Eds.; Chapman & Hall: London, 1989.
13. Mohit, S. M.; Tanushree, C. B.; Kanwal, S. Int J Biotechnol Appl 2011, 3, 41.
14. Garg, U. K.; Kaur, M. P.; Garg, V. K.; Sud, D. J Hazard Mater 2007, 140, 60.
15. Garg, U. K.; Kaur, M. P.; Garg, V. K.; Sud, D. Bioresour Technol 2008, 99, 1325.
16. Pateau, I.; Chen, C.-Z.; Jane, J. Ind Eng Chem Res 1994, 33, 1821.
17. Freeman, E. S.; Carroll, B. J Phys Chem 1958, 62, 394.
18. Friedman, H. L. J Polym Sci Part C: Polym Symp 1964, 6, 183.
19. Viboon, S.; Duangduen, A. J Anal Appl Pyrolysis 2009, 85, 155.
20. Dharmendra, B.; Parekh, Y. C. R.; Parimal, A.; Parikh, J. Renewable Sustainable Energy 2009, 1, 10.
21. Jacob, J.; Bhattacharya, M. Polym Int 1999, 48, 1165.
22. Swarna, S. P. M.; Satheesh Kumar, M. N.; Zahira, Y.; Siddaramaiah. In International Conference on Advances in Polymer Technology, Cochin University of Science and Technology: Cochin, Kerala, India, 2010; p 257.
23. Yam, K. L.; Gogoi, B. K.; Lai, C. C.; Selke, S. E. Polym Eng Sci 1990, 30, 693.
24. Selke, S.; Yam, K.; Nieman, K. Annual Technical Conference-Society of Plastics Engineers, New York, NY, USA, 1989, 1813.
25. Raj, R. G.; Kokta, B. V.; Maldas, D.; Daneault, C. J Appl Polym Sci 1989, 37, 1089.
26. Arvanitoyannis, I.; Biliaderis, C. G.; Ogawa, H.; Kawasaki, N. Carbohydr Polym 1998, 36, 89.
27. Obuz, E.; Herald, T. J.; Rausch, K. Cereal Chem 2001, 78, 97.
28. Karmaker, A. C.; Hoffmann, A.; Hinrichsen, G. J Appl Polym Sci 1994, 54, 1803.
29. Karmaker, A. C. J Mater Sci Lett 1997, 16, 462.
30. Rana, A. K.; Mandal, A.; Mitra, B. C.; Jacobson, R.; Rowell, R.; Banerjee, N. J Appl Polym Sci 1998, 69, 329.
31. Stefani, P. M.; Garcia, D.; Lopez, J.; Jimenez, A. J Therm Anal Calorim 2005, 81, 315.
32. Bakare, I. O.; Okieimen, F. E.; Pavithran, C.; Abdul Khalil, H. P. S.; Brahmakumar, M. Mater Des 2010, 31, 4274.
33. Caballero, J. A.; Conesa, J. A.; Font, R.; Marcilla, A. J Anal Appl Pyrolysis 1997, 42, 159.
34. Jakab, E.; Varhegyi, G.; Faix, J. O. J Anal Pyrolysis 2000, 56, 273.
35. Zhou, L.; Wang, Y.; Huang, Q.; Cai, H. Fuel Process Technol 2006, 87, 963.
36. Yogesh, C. R.; Parimal, A. P. Korean J Chem Eng 2011, 28, 788.
37. Ramiah, M. V. J Appl Polym Sci 1970, 14, 1323.
38. Sharma, K.; Ahmaruzzaman, M. Energy Fuels 2007, 21, 891.
39. Sorum, L.; Gronli, M. G.; Hustad, J. E. Fuel 2001, 80, 1217.
40. Hee, T.; Sea, C. J. Ind Eng Chem 2005, 11, 648.
41. Zhou, L.; Wang, Y.; Huang, Q.; Cai, J. Fuel Process Technol 2006, 87, 963.
42. Aboulkas, A.; El Harfi, K.; El Bouadili, A.; Nadifiyine, M.; Benchanaa, M. J Therm Anal Calorim 2009, 96, 883.
43. Aboulkas, A.; El Harfi, K.; Nadifiyine, M.; El Bouadili, A. J Therm Anal Calorim 2008, 91, 737.
44. Oasmaa, A.; Kuoppala, E.; Gust, S.; Solantausta, Y. Energy Fuels 2002, 17, 1.
45. Satheesh Kumar, M. N.; Zahira, Y.; Siddaramaiah. J Appl Polym Sci 2009, 114, 467.
46. Ceamanos, J.; Mastral, J. F.; Millera, A.; Aldea, M. E. J Anal Appl Pyrolysis 2002, 65, 93.
47. John, J.; Bhattacharya, M. Polym Int 1999, 48, 1165.
48. Macromolecular Physics; Wunderlich, B., Ed.; Academic: New York, 1978.
49. Yao, F.; Wu, Q.; Lei, Y.; Xu, Y. Ind Crops Prod 2008, 28, 63.
50. Jia, S.; Zhang, Z.; Wang, Z.; Zhang, X.; Du, Z. Polym Int 2005, 54, 320.
51. Price, D.; Anthony, G.; Carty, P. In Fire Retardant Materials; Horrocks, A. R., Price, D., Eds.; Woodhead: Cambridge, England, 2002.
52. Pering, G. A.; Farrell, P. V.; Springer, G. S. J Compos Mater 1989, 14, 54.
53. Mourtiz, A. P.; Gibson, A. G. In Fire Properties of Polymer Composite Materials; Gladwell, G. M. L., Ed.; Springer: Dordrecht, The Netherlands, 2006; Chapter 3.
54. Alcantaraa, G. B.; Barison, A.; Santos, M. D. S.; Santos, L. P. S.; de Toledo, J. F. F.; Ferreira, A. G. Orbital Elec J Chem Campo Grande 2010, 2, 41.
55. Zahira, Y.; Satheesh Kumar, M. N.; Kamaruddin, S. S. K.; Hilmi, M. N.; Khairul Zaman, H. M. J Thermoplast Compos Mater 2009, 3, 447.
56. Arib, R. M. N.; Sapuan, S. M.; Ahmad, M. M. H. M.; Paridah, M. T.; Khairul Zaman, H. M. D. Mater Des 2006, 27, 391.